AGU ADVANCING EARTH AND SPACE SCIENCES

Geophysical Research Letters®

RESEARCH LETTER
10.1029/2023GL102840

The Effect of Arctic Sea-Ice Loss on Extratropical Cyclones

Stephanie Hay[1], Matthew D. K. Priestley[1], Hao Yu[1], Jennifer L. Catto[1], and James A. Screen[1]

[1]Department of Mathematics and Statistics, University of Exeter, Exeter, UK

Key Points:

- The Northern Hemisphere winter storm tracks shift south and/or east in response to Arctic sea-ice loss
- Sea ice loss leads to fewer, slower, longer lasting, and weaker wintertime cyclones
- Responses are small compared to internal variability, but larger in winter than summer

Supporting Information:

Supporting Information may be found in the online version of this article.

Correspondence to:

S. Hay,
s.e.hay@exeter.ac.uk

Citation:

Hay, S., Priestley, M. D. K., Yu, H., Catto, J. L., & Screen, J. A. (2023). The effect of Arctic sea-ice loss on extratropical cyclones. *Geophysical Research Letters*, *50*, e2023GL102840. https://doi.org/10.1029/2023GL102840

Received 12 JAN 2023
Accepted 3 AUG 2023

Author Contributions:

Conceptualization: Stephanie Hay, Jennifer L. Catto, James A. Screen
Data curation: Stephanie Hay
Formal analysis: Stephanie Hay, Hao Yu
Funding acquisition: Jennifer L. Catto, James A. Screen
Investigation: Jennifer L. Catto
Methodology: Stephanie Hay, Matthew D. K. Priestley, Jennifer L. Catto, James A. Screen
Project Administration: James A. Screen
Resources: Hao Yu, Jennifer L. Catto
Software: Matthew D. K. Priestley
Supervision: Jennifer L. Catto, James A. Screen
Visualization: Stephanie Hay
Writing – original draft: Stephanie Hay

Abstract Taking advantage of the Polar Amplification Model Intercomparison Project simulations and using a Lagrangian objective feature tracking algorithm, we determine the response of extratropical cyclones to sea-ice loss and consequent weakening of the equator-to-pole near-surface temperature gradient. The wintertime storm tracks are found to shift equatorward in the North Atlantic and over Europe, and eastward in the North Pacific. In both regions, cyclones become weaker and slower, particularly on the poleward flank of the storm tracks. On average, there are fewer individual cyclones in the extratropics each winter, they last longer, are weaker, and travel more slowly. These changes are greatest over the Arctic, but still statistically significant in midlatitudes despite being small compared to internal variability. Inter-model spread in cyclone responses are not strongly correlated with that in Arctic warming or Arctic amplification. Little change in summertime cyclones is found.

Plain Language Summary Using identically performed experiments from eight different climate models, we study how low pressure systems, known as cyclones or storms, may change as Arctic sea ice diminishes. An algorithm is used to identify the weather systems and track them across their lifecycle. In the wintertime, the typical path of storms over the Atlantic Ocean shifts southward toward the equator. Over the Pacific, the storm tracks shifts toward North America. Arctic sea-ice loss causes there to be fewer storms each winter across the northern midlatitudes, and these tend to be weaker, slower moving, but longer lasting. These changes are largest over the Arctic itself but also found over mid-latitudes. These changes may be important because the number, location, and character of storms control the winter weather over Europe, North America and Asia. In the summertime, we did not find any detectable impact of Arctic sea-ice loss on storms.

1. Introduction

Arctic sea-ice loss, one of the most visible manifestations of greenhouse warming (e.g., Stroeve et al., 2012; Stroeve & Notz, 2018), and its global impacts (e.g., Barnes & Screen, 2015; Overland & Wang, 2010; Screen et al., 2018; Screen & Simmonds, 2013) have been studied extensively. The latest generation of climate models robustly project a continued reduction in the sea-ice extent over the coming decades (Notz et al., 2020). Locally, it is well understood that a loss of sea-ice has warmed and moistened the high-latitude atmosphere (Screen & Simmonds, 2010). There is, however, a less clear picture of the more remote impacts of sea-ice loss, particularly in the Northern Hemisphere mid-latitudes (Cohen et al., 2020; Overland et al., 2015).

Two ways in which sea-ice loss is theorized to impact the mid latitudes are by altering the speed and/or path of the midlatitude eddy-driven jet, and by weakening surface baroclinicity. Each of these effects arises as a consequence of Arctic Amplification (AA), whereby the northern high latitudes warm more rapidly than the lower latitudes (Serreze et al., 2008). Sea-ice loss is understood to be an important contributor to AA (Dai, 2019; Kumar et al., 2010; Screen & Simmonds, 2010) mainly through positive radiative feedbacks (Feldl et al., 2020; Pithan & Mauritsen, 2014; Schweiger et al., 2008). This preferential warming of the Arctic relative to lower latitudes decreases the meridional temperature gradient, which reduces surface baroclinicity and can weaken the upper-level westerlies via the thermal wind relation.

A potential impact of the weakening temperature gradients could be on the formation and maintenance of extratropical cyclones, which grow through baroclinic instability (Eady, 1949), and on the speed and lifecycle of these storms because the jet stream acts to guide surface cyclones. Climatologically, surface cyclones are organized into storm tracks over the North Pacific and Atlantic basins (Blackmon, 1976), as well as over the Mediterranean and Siberia (Blackmon et al., 1977; Hoskins & Hodges, 2002).

Writing – review & editing: Stephanie Hay, Matthew D. K. Priestley, Hao Yu, Jennifer L. Catto, James A. Screen

Via energetic constraints, the storm tracks can be expected to weaken if midlatitude eddies need no longer transport as much energy northward due to the change in equator-to-pole temperature gradient (Barpanda & Shaw, 2017; Shaw & Voigt, 2016). Evidence for weakening Northern Hemisphere storm tracks in reanalysis products has been attributed to AA (e.g., Coumou et al., 2015; Wang et al., 2017), and differences in the equator-to-pole temperature gradients can help explain some projected changes to the storm tracks in climate models (Harvey et al., 2014). However, a review by Shaw and Voigt (2016) outlined the difficulties in projecting changes to the storm tracks because of competing effects of the temperature gradients, and the complexity of factors affecting cyclones (Catto et al., 2019).

Using an ensemble of coordinated Polar Amplification Model Intercomparison Project (PAMIP) experiments (Smith et al., 2017), we explicitly track the response of extratropical cyclones to Arctic change isolated from other concurrent climate forcings. We seek to determine how cyclone characteristics are affected by sea-ice loss and examine inter-model differences under a consistent framework, whereas previous studies have focused on the aggregate storm tracks and have been limited to single-model studies.

2. Methods and Data

2.1. Feature Tracking

The method of Hodges (1994, 1995, 1999) is used to identify and track extratropical cyclones. Prior to tracking, the six-hourly sea-level pressure (*psl*) or 850 hPa relative vorticity (ξ_{850}) data are first spectrally filtered to remove wavenumbers smaller than 5 and larger than 63 for *psl*, or larger than 42 for ξ_{850}, in order to eliminate planetary waves and to capture only the synoptic scales. After the data are truncated to T63 or T42, cyclones are identified via grid-point extrema and then interpolated using B-spline interpolation and steepest gradient maximization. Tracks are generated via a nearest-neighbor approach and then optimized using a cost function, and only those longer than 1000 km and lasting for at least 48 hr are retained for analysis. For more details of the tracking method and its implementation, see Hoskins and Hodges (2002).

Using either *psl* or ξ_{850} as the tracking variable is common in the literature as there are benefits to each. Relative vorticity tends to detect cyclones earlier in their lifecycle and is not as sensitive to changes in the background state (Hoskins & Hodges, 2002). However, *psl* is a more commonly saved output at high temporal frequency in climate model experiments, including PAMIP. We present the *psl* tracking in the main manuscript but also investigate sensitivity to tracking variable and provide those results in Supporting Information S1.

Statistics of the features tracked by the algorithm are computed as in Hodges (1996) using spherical kernel estimators. Track density is defined as the number of tracks per month that pass through a 5° spherical cap. Other mean cyclone attributes (speed and intensity) are calculated using all information for the tracks passing through the spherical cap area and then the output is gridded. To examine individual tracks, we count the number of tracks over a season and then determine the average speed of individual cyclones using the Haversine formula to determine distance traveled in each timestep. We also compute, for each track, the average intensity (taken to be the magnitude of the spectrally filtered central pressure anomaly averaged over its whole lifecycle), and its lifetime. For regional statistics, we require at least 50% of the cyclone's lifecycle to be within the defined region. As such, there is no double-counting as our regions are non-overlapping.

2.2. PAMIP Tier 1 Experiments

The PAMIP experimental protocol is covered in detail in Smith et al. (2019), so here we give only a brief overview of the specific experiments used. Experiments 1.1 (*pdSST-pdSIC*) and 1.6 (*pdSST-futArcSIC*) consist of at least 100 ensemble members of 14-month-long atmosphere-only time-slice climate model simulations whereby a seasonal cycle of monthly mean sea-surface temperature (SST) and sea-ice concentration (SIC) is used (Figure S1 in Supporting Information S1 and Smith et al., 2019, Figures 5 and 6). In *pdSST-pdSIC*, these boundary conditions are obtained from observations over the period 1979–2008 from the Hadley Center Ice and Sea Surface Temperature data set (HadISST; Rayner et al., 2003). For *pdSST-futArcSIC*, the SIC over the Arctic is derived using quantile regression from the ensemble mean of the CMIP5 models, constrained by observations, from the 30-year period where they reach 2°C warming relative to the pre-industrial period (Smith et al., 2019, Appendix A). Where sea ice is lost, SSTs are also taken from future projections, while elsewhere they are identical to

the present-day experiment. Responses to sea-ice loss are calculated as the ensemble-mean difference between *pdSST-futArcSIC* and *pdSST-pdSIC*. Statistical significance is determined from a two-sided Student's *t*-test and refined using the false discovery rate following Wilks (2016) for a global significance of $\alpha_{global} = 0.1$.

For the feature tracking algorithm, we require six-hourly output of either *psl* or 850 hPa zonal (*ua*) and meridional velocity, from which we calculate ξ_{850}. The results we present in the main body of this paper use *psl* to perform the tracking as we were able to get the required model output from eight different models (CanESM5, CESM2, CNRM-CM6-1, EC-Earth3, HadGEM3-GC31-MM, IPSL-CM6A-LR, NorESM2-LM, TaiESM1). It is known that the response to sea-ice loss has a low signal-to-noise ratio (Peings et al., 2021; Screen et al., 2014), so we seek to use the largest number of models and ensemble members for testing significance and spread. However, we have also performed tracking with ξ_{850} using output from four of these models (CanESM5, CNRM-CM6-1, HadGEM3-GC31-MM, TaiESM1). For the maximum Eady growth rate (EGR) calculation for measuring baroclinic instability, daily *ua*, geopotential height, and temperature are required at 850 and 250 hPa:

$$EGR = 0.3098 \frac{|f|}{N} \left| \frac{\partial u}{\partial z} \right|, \quad (1)$$

where the Brunt-Vaisala frequency $N = \sqrt{g/\theta \times \partial\theta/\partial z}$, f is the Coriolis parameter, and $|\partial u/\partial z|$ is the vertical shear of zonal wind. Sufficient temporal resolution of these variables was available only for a subset of models for which *psl* tracking was performed (CanESM5, CESM2, CNRM-CM6-1, HadGEM3-GC31-MM, IPSL-CM6A-LR). For more information on the models used in this study, see Table S1 in Supporting Information S1. The latest generation of models has been shown to have improved representation of extratropical storm tracks compared to the previous generation, due to improved model resolution and physics (Harvey et al., 2020; Priestley et al., 2020).

The number of ensemble members provided from each model varies between 100 and 300, so we average the members across the models before calculating the multi-model ensemble mean so each model is given equal weight. Models differ in their physical parameterizations as well as their vertical and horizontal resolution. As the experiments are performed with identical boundary forcing, and the data are spectrally filtered for the tracking algorithm, results are directly comparable between models.

3. Results

3.1. Changes in the Large-Scale Environment

First, we quantify the changes in surface and lower tropospheric equator-to-pole temperature gradients in response to sea-ice loss, by examining the December–January–February (DJF) multi-model mean change in zonal-mean temperature (Figure 1a) and its meridional gradient (Figure 1b). The surface forcing is shown by the zonal-mean change in SIC in Figure 1a, lower panel, and the zonal-mean change in SST in Figure 1b, lower panel. Warming north of 45°N and from the surface up to 600 hPa results in a decrease in the temperature gradient between 40 and 80°N. At the surface, the present-day temperature gradient maxima are found near 40 and 60°N, the former of which is where the maximum SST gradient is found (Figure 1b, lower panel). The latter is nearly co-located with the region of largest weakening in response to sea-ice loss. The weakening gradient extends upward throughout the troposphere; at these high altitudes, the maximum response is located poleward of the maximum present-day gradient. The multi-model mean warming of the polar stratosphere also results in a decreasing temperature gradient aloft; however, there is large model spread in the sign of the temperature response here, as was shown in Screen et al. (2022) and Smith et al. (2022). Two models simulate stratospheric cooling (CNRM-CM6-1 and IPSL-CM6A-LR), while the rest simulate warming.

A vertically- (pressure-) weighted average of temperature over the lower troposphere reveals that the North Pacific (Figure 1c) exhibits two maxima in its warming profile, 0.4°C at 60°N and 0.6°C at 90°N. This pattern is more or less found in each of the models. For reference, the summertime (June–July–August [JJA]) warming is much smaller, around 0.1°C (dashed lines in Figures 1c and 1e). The resulting decrease in wintertime lower tropospheric meridional temperature gradient is located poleward of the maximum gradient (35°N in the Pacific). The meridional temperature gradient response is negative between 40 and 60°N and above 70°N with a magnitude of −0.03°C per degree of latitude. On the other hand, The North Atlantic (Figure 1e) exhibits one peak in warming of 0.8°C at 65°N and another of 0.7°C at 85°N, and has a larger meridional temperature gradient response in the

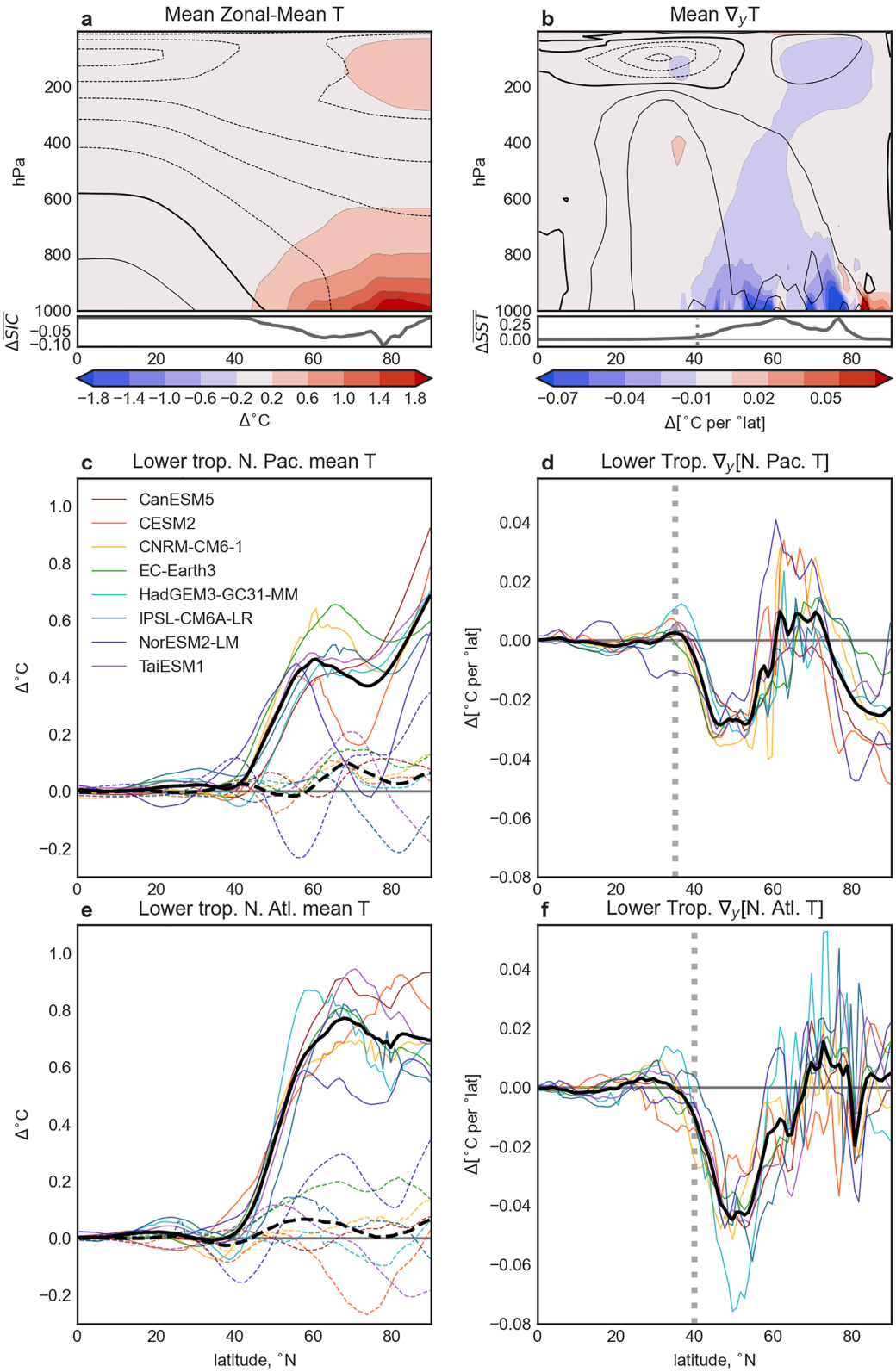

Figure 1.

lower troposphere (Figure 1f). As in the Pacific, the response is poleward of the maximum gradient, (40°N in the Atlantic). The maximum response is −0.04°C per degree of latitude near 50°N, however the signal at high latitudes is less clear due to significant model spread.

These results confirm and quantify the decrease in temperature gradients, which would be expected to reduce baroclinicity, in response to sea-ice loss. Separately, Screen et al. (2022) and Smith et al. (2022), found a significant equatorward shift of the eddy-driven jet in the same PAMIP experiments. In the remainder of this study, we build on these previous studies by examining the effect of simulated changes in the large-scale environment on extratropical cyclones.

3.2. Change in Extratropical Cyclones

The multi-model mean climatological distribution of cyclone track density in the present-day experiment shows cyclone tracks with maxima in the ocean basins, in North America, Siberia, and in the Mediterranean (Figure 2a). Robustly across all models, the storm tracks shift generally equatorward over the Atlantic and Europe, in response to sea-ice loss (Figure 2b), in good agreement with the response in EGR (Figure 2d). In the Pacific, the shift is more zonal, from the Western Pacific toward North America, despite a meridional shift in EGR. The greater shift over the eastern portion of the storm tracks suggests that changes are more pronounced in the later evolution of the cyclones than in their genesis regions.

Cyclones are at their maximum speed and intensity over the western half of the ocean basins (Figures 2e and 2g). Propagation speeds largely decrease on the poleward flank of the storm tracks and over the Arctic in response to sea-ice loss (Figure 2f). On the equatorward flank of the Pacific, Atlantic, and Mediterranean storm tracks, cyclones increase in speed, indicating again a shift in the storm tracks. Generally, cyclones are found to weaken in a pattern corresponding to that of the EGR (Figures 2d and 2h) except for on the eastern coast of the continental landmasses, where a clear strengthening is found, perhaps related to land-sea contrasts. However, because SSTs are imposed in the models, the magnitude of land-sea contrasts are exaggerated in an unphysical way.

We find little dependence on tracking variable when comparing across the same models (Figure S2 in Supporting Information S1). This is particularly true for the track density and speed responses. There is less evidence for weakening storms when tracking with ξ_{850}, but comparison is limited due to different measures of intensity.

Examining individual cyclones, we average over the midlatitudes, the Arctic, the North Atlantic, and the North Pacific to determine the mean change to cyclones in that region (Figure 3). In the multi-model mean, the results largely confirm those shown in Figure 2: fewer, weaker, and slower-moving cyclones are found in response to sea-ice loss in all regions, with the greatest responses found over the Arctic. Changes in peak intensity mirror those of average intensity (not shown). Additionally, Figure 3d shows that the majority of models find that individual cyclones have a longer lifetime, particularly in the Arctic.

However, we find large model spread in some statistics. For example, the median response across all models is 1 fewer storms per season over the midlatitudes, but in NorESM2-LM we find on average 2 more storms, and in EC-Earth3 there are 2 fewer storms (Figure 3a). As we count fewer cyclones in the Atlantic and Pacific in all models (Figure 3a), we conclude that the increase in cyclones in some models are found over the continents or the Mediterranean.

The larger decrease in temperature gradient in the Atlantic sector compared to the Pacific is not reflected in the change in number of cyclones, which is similar in the two basins. However, cyclones in the Atlantic generally slow more (Figure 3b), weaken more (Figure 3c) and increase their lifetime (Figure 3d) more than those in the Pacific.

There is no clear inter-model relationship between any of the statistics and the magnitude of the temperature gradient decrease, for example, HadGEM3-GC31-MM has the largest decrease in the gradient in the Atlantic, but

Figure 1. (a) The multi-model-mean zonal-mean DJF warming response (upper), and change in sea-ice concentration (lower). (b) The meridional temperature gradient response (upper), and the difference in sea-surface temperature forcing (lower). Black contours in (a) and (b) show the present day climatologies, where solid contours are positive values and dotted contours are negative values, with the zero contour being thicker. (c) Zonal-mean lower tropospheric (925–700 hPa average) temperature response over the North Pacific, where each colored line is a different model and the black line is the multi-model mean. Solid lines are for winter and dashed lines for summer. (d) As (c), but for the meridional temperature gradient. (e, f) As (c, d) but for the North Atlantic. The thick dotted gray lines in (b), lower panel, (d), (f) indicate the latitude of the maximum present-day temperature gradient.

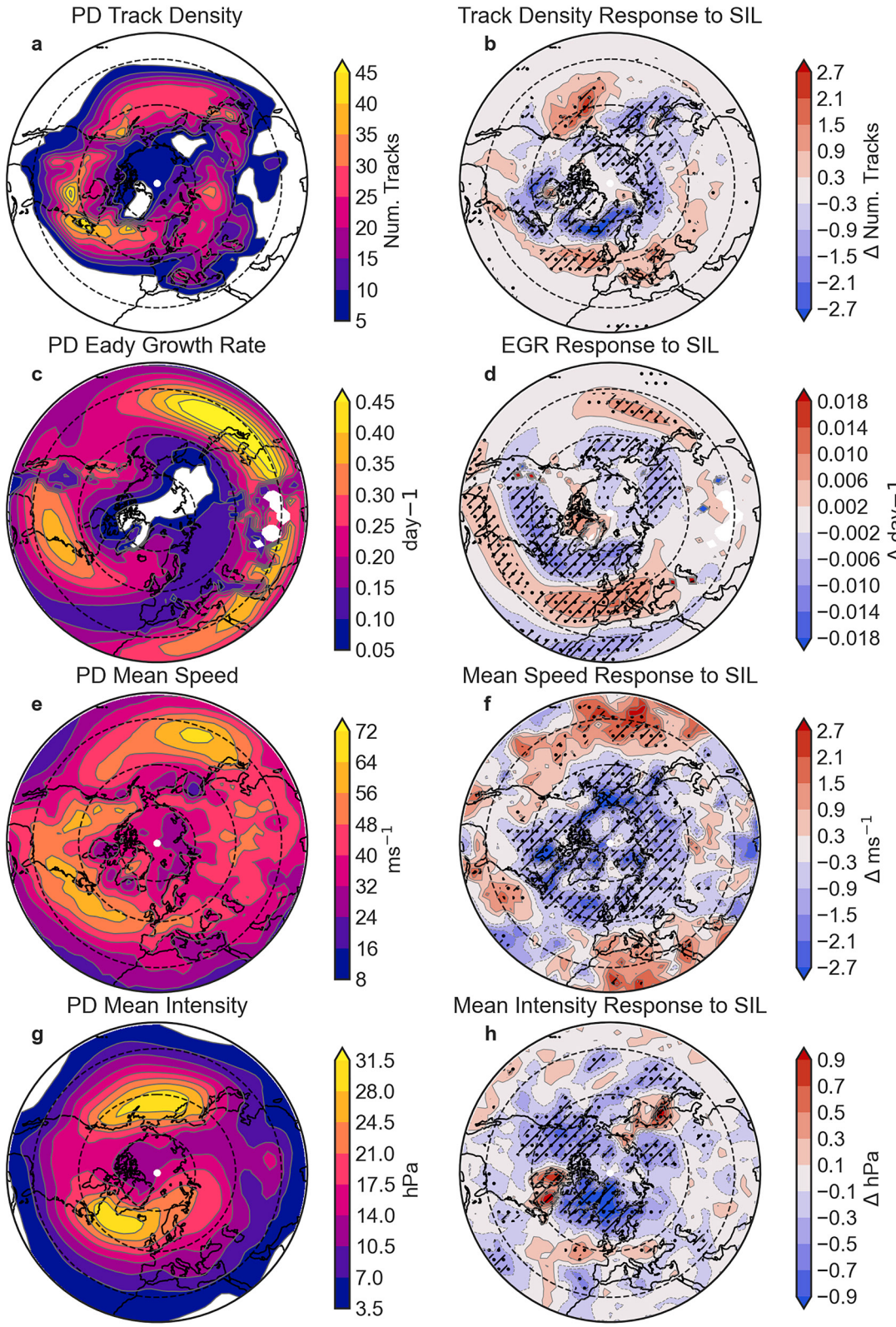

Figure 2. (a) The present-day multi-model winter cyclone track density, as determined by *psl* tracking, measured in number of tracks per month per 5° spherical cap. (b) The multi-model mean cyclone track density response. (c) The present-day five-model-subset mean Eady growth rate (EGR). (d) The five-model-subset mean response of the EGR. (e, f) As (a, b) but for mean propagation speed. (g, h) As (a, b) for mean cyclone intensity. Stippling indicates the multi-model mean response is significant at the 95% confidence level, and hatching indicates where $p < p_{FDR} \approx 0.01$.

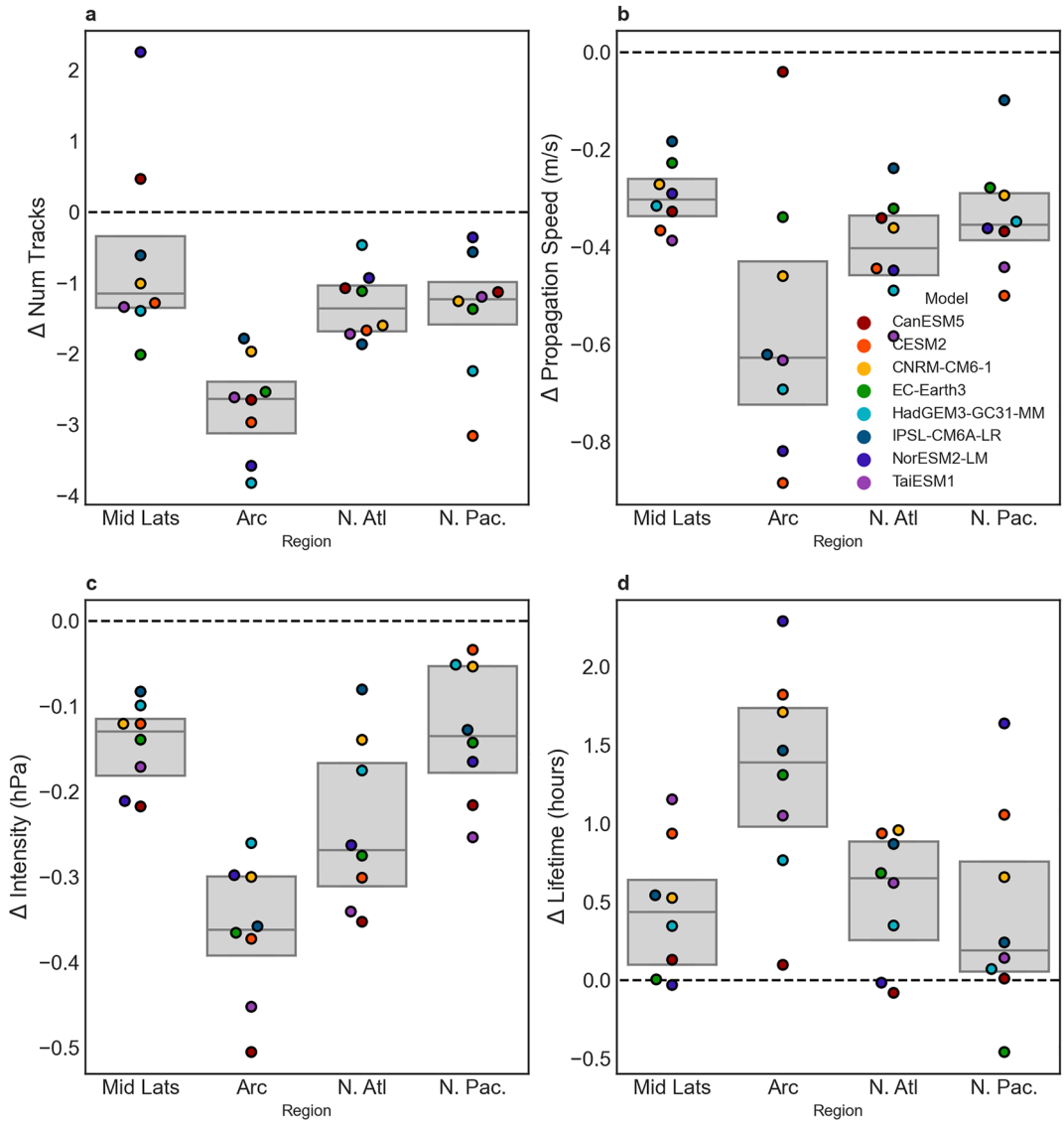

Figure 3. (a) The difference in number of tracks counted over a winter season in the midlatitudes (30–70°N), Arctic (>70°N) and midlatitude North Atlantic (230–350°) and North Pacific (130–230°). Dots indicate individual model responses while gray boxes show the inter-quartile range of the distribution, centered on the median of the model response. (b) As (a) but for mean cyclone speed. (c) As (a) but for mean cyclone intensity. (d) As (a) but for mean cyclone lifetime.

is not an outlier in any of the statistics there. There is 13–19 times more warming at the Arctic surface than globally, and 8–16 times more warming in the Arctic than globally in the lower troposphere, 925–700 hPa, in these models as a result of sea-ice loss. These values of AA are very high compared to estimates from observations and CMIP6 experiments (Rantanen et al., 2021) because the global mean change is small, by design. However, we do not find any statistically significant relationships across models in number, intensity, or lifetime of midlatitude cyclones with the magnitude of Arctic warming or global warming, or with AA (e.g., Figure S4 in Supporting Information S1). We note that there is no relationship between the different cyclone metrics either; the model with the greatest decrease in propagation speed is not necessarily that which weakens most, for example. This may indicate a large role for internal variability within the response of cyclones to sea-ice loss.

It is Arctic cyclones that experience the greatest response to sea-ice loss: on average we find about three fewer storms per season, they slow by 0.6 m/s, weaken by 0.35 hPa, and last 1.5 hr longer. However, these represent only small changes compared to the present day climatologies: 5%, 3%, 2%, and 1%, respectively. Relative changes in the midlatitudes are even smaller, and responses are smaller than the member-to-member variability within

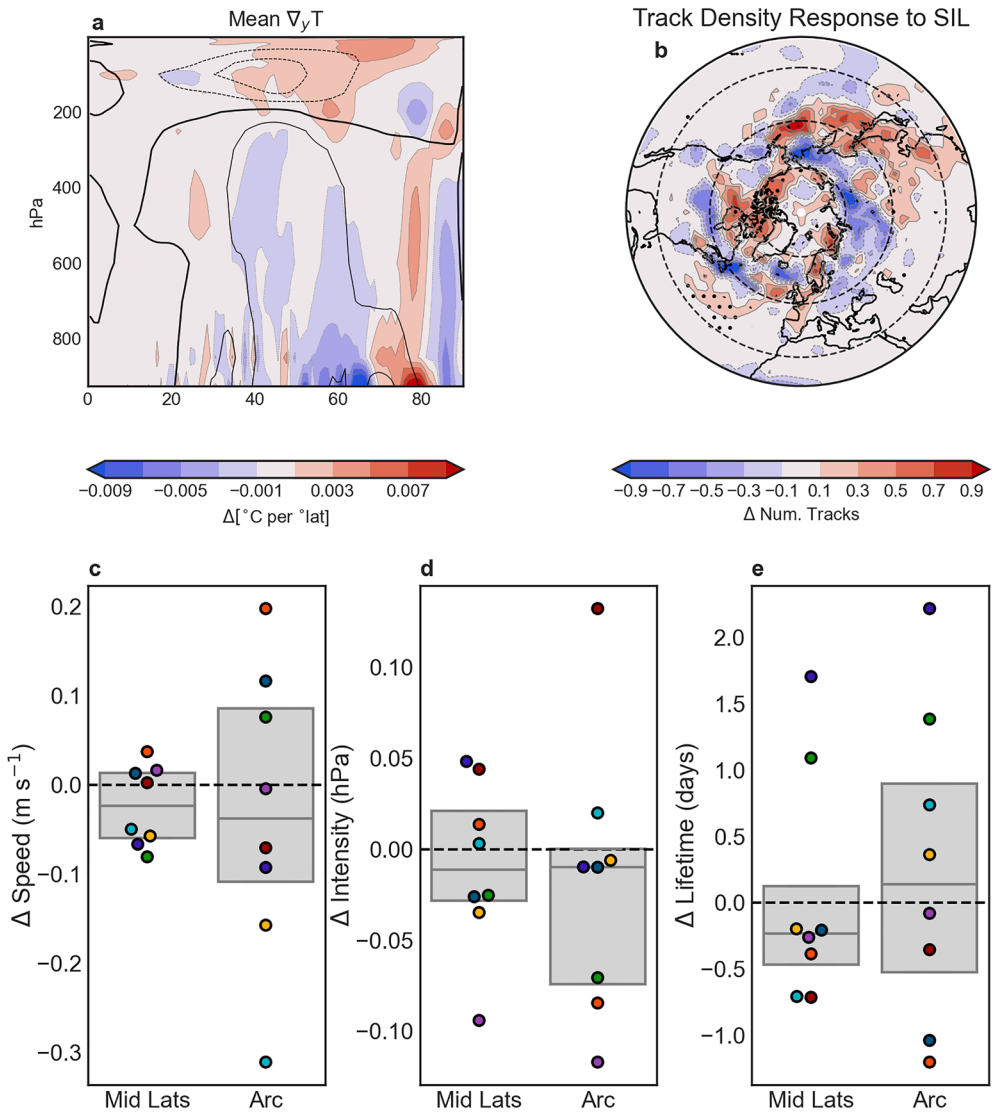

Figure 4. (a) The summer multi-model-mean change in zonal-mean meridional temperature gradient (filled contours) and present-day climatology (black contours). (b) Summer cyclone track density response to sea-ice loss. Stippling indicates the response is significant at the 95% confidence level. (c) Mean change in summer cyclone speed over midlatitudes and the Arctic. Dots indicate individual model responses while gray boxes show the inter-quartile range of the distribution, centered on the median. (d) As (c) but for mean cyclone intensity. (e) As (c) but for mean cyclone lifetime.

a model. As with midlatitude cyclones, we do not find any relationship between the amount of warming or AA and the inter-model spread in Arctic cyclone statistics. One caveat is that the tracking algorithm is optimized for midlatitude synoptic-scale cyclones and not necessarily for Arctic cyclones which have smaller spatial scales. However, similar parameter settings in previous studies of Arctic cyclones and have found good agreement with reanalysis (e.g., Day et al., 2018).

3.3. Seasonal Differences

We carried out a similar analysis for summertime cyclones. Changes in the meridional temperature gradient (Figure 4a) are negative over the high Arctic, positive between 70 and 85°N, and then negative from 50 to 70°N. The change in the gradient is an order of magnitude smaller than in winter. The summertime storm tracks are shifted poleward compared to the wintertime (Figure S3a in Supporting Information S1) and the resulting response in track density is noisy and not statistically significant (Figure 4b) when controlling for the false discovery rate.

Examining individual cyclones, there is little signal to be found as responses are small and the inter-model spread is large, particularly for Arctic cyclones. We can conclude that, under this sea-ice loss protocol, there is little to no robust change in cyclone tracks in summertime. It is possible that the summertime response is driven by other factors not included here, such as remote ocean warming or air-sea interactions (Kang et al., 2023).

4. Discussion and Conclusions

In recent years, modeling studies have shown that the response to sea-ice loss in the midlatitudes is generally small compared to internal climate variability and relative to the full effects of greenhouse warming. A consistent picture has nonetheless emerged: a small but significant weakening of the circulation (Smith et al., 2022). Reconciling modeling studies with observations remains difficult and statistical relationships indicate the effect could be larger than models have found (Cohen et al., 2020). This could be attributable to the use of atmosphere-only models, shown to underestimate the responses compared to fully coupled models (Deser et al., 2015), but recent work has also found evidence of spurious warming in coupled sea-ice loss simulations (England et al., 2022). Furthermore, the response to sea-ice loss may potentially be impacted by known issues with the signal-to-noise ratio in models (Scaife & Smith, 2018; Screen et al., 2022; Smith et al., 2022). Finally, observational studies are not able to disentangle the various causes of AA, which has components that arise independently of sea-ice loss (Pithan & Mauritsen, 2014). Regardless, the responses found here are possibly an underestimate of the true response due to the lack of coupling (with the caveat presented above), or due to a too-weak eddy feedback found in these same experiments (Screen et al., 2022; Smith et al., 2022), and could potentially therefore be understood to represent a lower bound.

A simple picture of a weakening equator-to-pole temperature gradient in response to sea-ice loss leading to a reduction and shift in the eddy-driven jet and in baroclinicity is consistent with the resulting large-scale mean impact on storms we have found here. However, some regional responses, such as the zonal shift in storm track density in the Pacific, are not captured by this simple picture, and further investigation is still required. Model spread in some statistics is quite large compared to the mean response, however, no simple metrics of warming or AA correlate with the model spread, and no obvious relationship is found with local decreases in the zonal-mean temperature gradient. Additionally, the two models that cool in the Arctic stratosphere on average do not exhibit different behavior to those that do not.

Other factors than meridional temperature gradients affect baroclinicity, such as changes to static stability (e.g., Priestley et al., 2022), and competing effects can be expected to impact cyclones, for example, changes in latent heating (Dolores-Tesillos et al., 2022) and vertical temperature gradients. Finally, cyclone response differences may be masked by internal variability and the storm track response may be dependent on the mean state, which differs between models. The model spread in the jet shift is strongly related to the strength of eddy feedback (Screen et al., 2022; Smith et al., 2022), so we might expect this to also manifest in the storm track response. More work is needed to understand which mechanisms affect the response of extratropical cyclone tracks to sea-ice loss, and how this leads to the inter-model variability we find.

The weak response in summertime is consistent with previous modeling studies, but might appear at odds with observational studies that have reported a weakening summertime circulation and hypothesized that this is a consequence of AA (Coumou et al., 2015, 2018). Whilst we find no clear response in the storm tracks, we also find little to no AA in response to sea-ice loss. In recent years, strong cyclones have been observed in the Arctic, and have been argued to be both the product and consequence of accelerating sea-ice loss (Simmonds & Keay, 2009; Vavrus, 2013). In the cold season too, more numerous and intense cyclones have been associated with a decreased ice cover (Valkonen et al., 2021). Despite an increase in moisture availability and baroclinicity, other studies have found no increase in cyclone numbers or intensity (Koyama et al., 2017). More work is required to understand these discrepancies.

Finally, sea-ice loss represents just one aspect of the global warming response. Previous work using the same cyclone tracking algorithm identified a very different response in the midlatitude storm tracks and cyclone intensity in CMIP6 future projections (Priestley & Catto, 2022). In the North Atlantic, opposing influences of sea-ice and ocean warming were found on the storm tracks (Yu et al., 2023), which may explain the difference. Future work will focus on placing the results presented here within the context of general greenhouse warming.

Overall, our results are consistent with other modeling studies: we find an impact of sea-ice loss on the Arctic and in the midlatitudes in wintertime, but the magnitude is small compared to internal variability. Together with

other concurrent forcings (e.g., remote ocean warming, aerosols) and the greenhouse warming response, there is a potential for the effects of sea-ice loss on dynamical changes to be masked. Nevertheless, we find that sea-ice loss in isolation results in fewer, slower, longer lasting, and weaker wintertime extratropical cyclones, and a southward and/or eastward shift of the storm tracks.

Data Availability Statement

The cyclone tracking algorithm TRACK is available from https://gitlab.act.reading.ac.uk/track/track. PAMIP output is publicly available through the Earth System Grid Federation (https://esgf-node.llnl.gov/projects/cmip6/).

Acknowledgments
J.A.S, S.H, and J.L.C were funded by Natural Environment Research Council Grant NE/V005855/1. M.D.K.P is funded by the Willis Research Network and H.Y. is funded by the China Scholarship Council. We thank Michael Sigmond at CCCma, Svenya Chripko and Rym Msadek at CERFACS, Xavier Levine and Pablo Ortega at BCS, Rosie Eade at Met Office UK, and Lise Seland Graff at NMI for providing us with the PAMIP output not publicly available.

References

Barnes, E. A., & Screen, J. A. (2015). The impact of Arctic warming on the midlatitude jet-stream: Can it? Has it? Will it? *Wiley Interdisciplinary Reviews: Climate Change*, *6*(3), 277–286. https://doi.org/10.1002/wcc.337

Barpanda, P., & Shaw, T. A. (2017). Using the moist static energy budget to understand storm-track shifts across a range of time scales. *Journal of the Atmospheric Sciences*, *74*(8), 2427–2446. https://doi.org/10.1175/jas-d-17-0022.1

Blackmon, M. L. (1976). A climatological spectral study of the 500 mb geopotential height of the northern hemisphere. *Journal of the Atmospheric Sciences*, *33*(8), 1607–1623. https://doi.org/10.1175/1520-0469(1976)0331607:acssot2.0.co;2

Blackmon, M. L., Wallace, J. M., Lau, N.-C., Lau, N.-C., Lau, N.-C., Lau, N.-C., & Mullen, S. L. (1977). An observational study of the northern hemisphere wintertime circulation. *Journal of the Atmospheric Sciences*, *34*(7), 1040–1053. https://doi.org/10.1175/1520-0469(1977)0341040:aosotn2.0.co;2

Catto, J. L., Ackerley, D., Booth, J. F., Champion, A. J., Colle, B. A., Pfahl, S., et al. (2019). The future of midlatitude cyclones. *Current Climate Change Reports*, *5*(4), 407–420. https://doi.org/10.1007/s40641-019-00149-4

Cohen, J., Zhang, X., Francis, J. A., Jung, T., Kwok, R., Overland, J. E., et al. (2020). Divergent consensuses on Arctic amplification influence on midlatitude severe winter weather. *Nature Climate Change*, *10*(1), 20–29. https://doi.org/10.1038/s41558-019-0662-y

Coumou, D., Capua, G. D., Vavrus, S., Wang, L., & Wang, S.-Y. (2018). The influence of Arctic amplification on mid-latitude summer circulation. *Nature Communications*, *9*(1), 2959. https://doi.org/10.1038/s41467-018-05256-8

Coumou, D., Lehmann, J., & Beckmann, J. (2015). The weakening summer circulation in the northern hemisphere mid-latitudes. *Science*, *348*(6232), 324–327. https://doi.org/10.1126/science.1261768

Dai, A., Luo, D., Song, M., & Liu, J. (2019). Arctic amplification is caused by sea-ice loss under increasing CO_2. *Nature Communications*, *10*(1), 121. https://doi.org/10.1038/s41467-018-07954-9

Day, J. J., Day, J. J., Day, J. W., Holland, M. M., & Hodges, K. I. (2018). Seasonal differences in the response of Arctic cyclones to climate change in CESM1. *Climate Dynamics*, *50*(9–10), 3885–3903. https://doi.org/10.1007/s00382-017-3767-x

Deser, C., Tomas, R. A., & Sun, L. (2015). The role of ocean–atmosphere coupling in the zonal-mean atmospheric response to Arctic sea ice loss. *Journal of Climate*, *28*(6), 2168–2186. https://doi.org/10.1175/jcli-d-14-00325.1

Dolores-Tesillos, E., Teubler, F., & Pfahl, S. (2022). Future changes in North Atlantic winter cyclones in CESM-LE – Part 1: Cyclone intensity, potential vorticity anomalies, and horizontal wind speed. *Weather and Climate Dynamics*, *3*(2), 429–448. https://doi.org/10.5194/wcd-3-429-2022

Eady, E. T. (1949). Long waves and cyclone waves. *Tellus A*, *1*(3), 33–52. https://doi.org/10.3402/tellusa.v1i3.8507

England, M. R., Eisenman, I., & Wagner, T. J. W. (2022). Spurious climate impacts in coupled sea ice loss simulations. *Journal of Climate*, *35*(22), 7401–7411. https://doi.org/10.1175/jcli-d-21-0647.1

Feldl, N., Po-Chedley, S., Singh, H. K. A., Hay, S., & Kushner, P. J. (2020). Sea ice and atmospheric circulation shape the high latitude lapse rate feedback. *NPJ Climate and Atmospheric Science*, *3*(1), 41. https://doi.org/10.1038/s41612-020-00146-7

Harvey, B., Cook, P. A., Shaffrey, L., & Schiemann, R. (2020). The response of the northern hemisphere storm tracks and jet streams to climate change in the CMIP3, CMIP5, and CMIP6 climate models. *Journal of Geophysical Research: Atmospheres*, *125*(23), e2020JD032701. https://doi.org/10.1029/2020jd032701

Harvey, B., Shaffrey, L., & Woollings, T. (2014). Equator-to-pole temperature differences and the extra-tropical storm track responses of the CMIP5 climate models. *Climate Dynamics*, *43*(5–6), 1171–1182. https://doi.org/10.1007/s00382-013-1883-9

Hodges, K. I. (1994). A general method for tracking analysis and its application to meteorological data. *Monthly Weather Review*, *122*(11), 2573–2586. https://doi.org/10.1175/1520-0493(1994)122<2573:agmfta>2.0.co;2

Hodges, K. I. (1995). Feature tracking on the unit sphere. *Monthly Weather Review*, *123*(12), 3458–3465. https://doi.org/10.1175/1520-0493(1995)123<3458:ftotus>2.0.co;2

Hodges, K. I. (1996). Spherical nonparametric estimators applied to the UGAMP model integration for AMIP. *Monthly Weather Review*, *124*(12), 2914–2932. https://doi.org/10.1175/1520-0493(1996)124<2914:sneatt>2.0.co;2

Hodges, K. I. (1999). Adaptive constraints for feature tracking. *Monthly Weather Review*, *127*(6), 1362–1373. https://doi.org/10.1175/1520-0493(1999)127<1362:acfft>2.0.co;2

Hoskins, B. J., & Hodges, K. I. (2002). New perspectives on the northern hemisphere winter storm tracks. *Journal of the Atmospheric Sciences*, *59*(6), 1041–1061. https://doi.org/10.1175/1520-0469(2002)059<1041:npotnh>2.0.co;2

Kang, J. M., Shaw, T., & Sun, L. (2023). Arctic sea ice loss weakens northern hemisphere summertime storminess but not until the late 21st century. *Geophysical Research Letters*, *50*(9), e2022GL102301. https://doi.org/10.1029/2022gl102301

Koyama, T., Stroeve, J., Cassano, J. J., & Crawford, A. D. (2017). Sea ice loss and Arctic cyclone activity from 1979 to 2014. *Journal of Climate*, *30*(12), 4735–4754. https://doi.org/10.1175/jcli-d-16-0542.1

Kumar, A., Perlwitz, J., Eischeid, J., Quan, X.-W., Xu, T., Zhang, T., et al. (2010). Contribution of sea ice loss to Arctic amplification. *Geophysical Research Letters*, *37*(21), e2010GL045022. https://doi.org/10.1029/2010gl045022

Notz, D., Dörr, J., Bailey, D. A., Blockley, E., Bushuk, M., Debernard, J., & Vancoppenolle, M. (2020). Arctic sea ice in CMIP6. *Geophysical Research Letters*, *47*(10), e2019GL086749. https://doi.org/10.1029/2019gl086749

Overland, J. E., Francis, J. A., Hall, R., Hanna, E., Kim, S.-J., & Vihma, T. (2015). The melting Arctic and midlatitude weather patterns: Are they connected?*. *Journal of Climate*, *28*(20), 7917–7932. https://doi.org/10.1175/jcli-d-14-00822.1

Overland, J. E., & Wang, M. (2010). Large-scale atmospheric circulation changes are associated with the recent loss of Arctic sea ice. *Tellus A*, *62*(1), 1. https://doi.org/10.1111/j.1600-0870.2009.00421.x

Peings, Y., Labe, Z., & Magnusdottir, G. (2021). Are 100 ensemble members enough to capture the remote atmospheric response to +2°c Arctic sea ice loss? *Journal of Climate*, *34*(10), 3751–3769. https://doi.org/10.1175/jcli-d-20-0613.1

Pithan, F., & Mauritsen, T. (2014). Arctic amplification dominated by temperature feedbacks in contemporary climate models. *Nature Geoscience*, *7*(3), 181–184. https://doi.org/10.1038/ngeo2071

Priestley, M. D. K., Ackerley, D., Catto, J. L., & Hodges, K. I. (2022). Drivers of biases in the CMIP6 extratropical storm tracks. Part 1: Northern hemisphere. *Journal of Climate*, *36*(5), 1451–1467. https://doi.org/10.1175/jcli-d-20-0976.1

Priestley, M. D. K., Ackerley, D., Catto, J. L., Hodges, K. I., McDonald, R. E., & Lee, R. (2020). An overview of the extratropical storm tracks in CMIP6 historical simulations. *Journal of Climate*, *33*(15), 6315–6343. https://doi.org/10.1175/jcli-d-19-0928.1

Priestley, M. D. K., & Catto, J. L. (2022). Future changes in the extratropical storm tracks and cyclone intensity, wind speed, and structure. *Weather and Climate Dynamics*, *3*(1), 337–360. https://doi.org/10.5194/wcd-3-337-2022

Rantanen, M., Karpechko, A. Y., Lipponen, A., Nordling, K., Hyvärinen, O., Ruosteenoja, K., et al. (2021). The Arctic has warmed four times faster than the globe since 1980. *Null*. https://doi.org/10.21203/rs.3.rs-654081/v1

Rayner, N., Parker, D., Horton, E. B., Folland, C. K., Alexander, L. V., Rowell, D. P., & Kaplan, A. (2003). Global analyses of sea surface temperature, sea ice, and night marine air temperature since the late nineteenth century. *Journal of Geophysical Research*, *108*(D14), 4407. https://doi.org/10.1029/2002jd002670

Scaife, A. A., & Smith, D. (2018). A signal-to-noise paradox in climate science. *NPJ Climate and Atmospheric Science*, *1*(1), 28. https://doi.org/10.1038/s41612-018-0038-4

Schweiger, A., Lindsay, R., Vavrus, S., & Francis, J. A. (2008). Relationships between Arctic sea ice and clouds during autumn. *Journal of Climate*, *21*(18), 4799–4810. https://doi.org/10.1175/2008jcli2156.1

Screen, J. A., Deser, C., Simmonds, I., & Tomas, R. A. (2014). Atmospheric impacts of Arctic sea-ice loss, 1979–2009: Separating forced change from atmospheric internal variability. *Climate Dynamics*, *43*(1–2), 333–344. https://doi.org/10.1007/s00382-013-1830-9

Screen, J. A., Deser, C., Smith, D., Zhang, X., Blackport, R., Kushner, P. J., et al. (2018). Consistency and discrepancy in the atmospheric response to Arctic sea-ice loss across climate models. *Nature Geoscience*, *11*(3), 155–163. https://doi.org/10.1038/s41561-018-0059-y

Screen, J. A., Eade, R., Smith, D. M., Thomson, S., & Yu, H. (2022). Net equatorward shift of the jet streams when the contribution from sea-ice loss is constrained by observed eddy feedback. *Geophysical Research Letters*, *49*(23), e2022GL100523. https://doi.org/10.1029/2022GL100523

Screen, J. A., & Simmonds, I. (2010). The central role of diminishing sea ice in recent Arctic temperature amplification. *Nature*, *464*(7293), 1334–1337. https://doi.org/10.1038/nature09051

Screen, J. A., & Simmonds, I. (2013). Exploring links between Arctic amplification and mid-latitude weather. *Geophysical Research Letters*, *40*(5), 959–964. https://doi.org/10.1002/grl.50174

Serreze, M. C., Barrett, A. P., Stroeve, J., Kindig, D. N., & Holland, M. M. (2008). The emergence of surface-based Arctic amplification. *The Cryosphere*, *3*(1), 11–19. https://doi.org/10.5194/tc-3-11-2009

Shaw, T. A., & Voigt, A. (2016). Understanding the links between subtropical and extratropical circulation responses to climate change using aquaplanet model simulations. *Journal of Climate*, *29*(18), 6637–6657. https://doi.org/10.1175/jcli-d-16-0049.1

Simmonds, I., & Keay, K. (2009). Extraordinary September Arctic sea ice reductions and their relationships with storm behavior over 1979–2008. *Geophysical Research Letters*, *36*(19), L19715. https://doi.org/10.1029/2009gl039810

Smith, D., Dunstone, N., Scaife, A. A., Fiedler, E., Copsey, D., & Hardiman, S. C. (2017). Atmospheric response to Arctic and Antarctic sea ice: The importance of ocean–atmosphere coupling and the background state. *Journal of Climate*, *30*(12), 4547–4565. https://doi.org/10.1175/jcli-d-16-0564.1

Smith, D., Eade, R., Andrews, M. B., Ayres, H., Clark, A., Chripko, S., et al. (2022). Robust but weak winter atmospheric circulation response to future Arctic sea ice loss. *Nature Communications*, *13*(1), 727. https://doi.org/10.1038/s41467-022-28283-y

Smith, D., Screen, J. A., Deser, C., Cohen, J., Fyfe, J. C., García-Serrano, J., et al. (2019). The polar amplification model intercomparison project (PAMIP) contribution to CMIP6: Investigating the causes and consequences of polar amplification. *Geoscientific Model Development*, *12*(3), 1139–1164. https://doi.org/10.5194/gmd-12-1139-2019

Stroeve, J., Kattsov, V. M., Barrett, A. P., Serreze, M. C., Pavlova, T., Holland, M. M., & Meier, W. N. (2012). Trends in Arctic sea ice extent from CMIP5, CMIP3 and observations. *Geophysical Research Letters*, *39*(16), e2012GL052676. https://doi.org/10.1029/2012gl052676

Stroeve, J., & Notz, D. (2018). Changing state of Arctic sea ice across all seasons. *Environmental Research Letters*, *13*(10), 103001. https://doi.org/10.1088/1748-9326/aade56

Valkonen, E., Cassano, J. J., & Cassano, E. N. (2021). Arctic cyclones and their interactions with the declining sea ice: A recent climatology. *Journal of Geophysical Research: Atmospheres*, *126*(12), e2020JD034366. https://doi.org/10.1029/2020jd034366

Vavrus, S. J. (2013). Extreme Arctic cyclones in CMIP5 historical simulations. *Geophysical Research Letters*, *40*(23), 6208–6212. https://doi.org/10.1002/2013gl058161

Wang, J., Kim, H.-M., & Chang, E. K. M. (2017). Changes in northern hemisphere winter storm tracks under the background of Arctic amplification. *Journal of Climate*, *30*(10), 3705–3724. https://doi.org/10.1175/jcli-d-16-0650.1

Wilks, D. S. (2016). "The stippling shows statistically significant grid points": How research results are routinely overstated and overinterpreted, and what to do about it. *Bulletin of the American Meteorological Society*, *97*(12), 2263–2273. https://doi.org/10.1175/bams-d-15-00267.1

Yu, H., Screen, J., Hay, S., Catto, J., & Xu, M. (2023). Winter precipitation responses to projected Arctic sea-ice loss and global ocean warming and their opposing influences over northeast Atlantic region. *Journal of Climate*, *36*(15), 4951–4966. https://doi.org/10.1175/jcli-d-22-0774.1